IOP Publishing Physica Scripta
Phys. Scr. 95 (2020) 045218 (9pp) https://doi.org/10.1088/1402-4896/ab68ff

Complex dynamics of coupled map lattices under random asynchronous updating

Mayurakshi Nag and Swarup Poria

Department of Applied Mathematics, University of Calcutta, 92, A.P.C Road, Kolkata-700009, India

E-mail: mayurakshimath@gmail.com

Received 25 October 2019, revised 25 December 2019
Accepted for publication 8 January 2020
Published 18 February 2020

Abstract

The effects of a new type of asynchronous updating on the dynamical behavior of coupled chaotic maps with nearest neighbor as well as global coupling are studied in this paper. In contrast to synchronous updating, the occurrence of the synchronized fixed point window is observed in the parameter space for nearest neighbor interactions as a consequence of asynchronous updating. Moreover, the effects of variation of the degree of asynchronocity have been investigated and it is observed that the size of the synchronized fixed point window strongly depends on the degree of asynchronocity. The value of coupling constant at the point of onset of synchronization is found analytically and the result is in good agreement with the numerics. Lattice size also has a significant impact on the synchronization behavior for some coupling function. On the other hand in a globally coupled network, synchronization is identified for a certain range of the degree of asynchronocity but surprisingly the width of synchronized fixed point window is independent of the value of the asynchronocity parameter. This study may be useful to explain the spatiotemporal order structure observed in spatially extended complex biological and social systems with the help of stochastic asynchronous updating.

Keywords: synchronization, coupled map lattice, asynchronous updating

(Some figures may appear in colour only in the online journal)

1. Introduction

Coupled map lattice (CML) captures essential features of emergent synchrony in extended dynamical systems consisting of interacting nonlinear units [1]. It has been studied as a model of spatiotemporal phenomena in various fields like condensed matter physics, neuroscience [2, 3], chemical physics, laser theory [4], communications [5] and even in evolutionary biology [6]. CMLs can be constructed from deterministic cellular automata (CAs) [7], which itself has attracted huge attention in research area last decade [8, 9].

The spatiotemporal behavior arises from two competent mechanisms typically the nonlinear dynamics of the local maps and the diffusion due to the coupling. Nearest neighbor interaction in CML can show rich phenomenology like spatial pattern and intermittent behavior [10]. But due to weakness in coupling effect, nearest neighbor coupling is not capable of generating synchronized orbit in CML of chaotic maps.

In globally coupled maps, for weaker coupling, cluster formation can be identified and with the increasing coupling strength different types of phases like coherent and turbulent appear. Global coupling has practical implications in the fields like gas discharges, transport process in semi-conductors [11] and also in Josephson junction array [12], multimode lasers and biological information processing, neurodynamics, oscillating chemical reactions [13], evolutionary dynamics [14].

Synchronization, more specifically chaos synchronization in a network of coupled nonlinear system has become a widely recognized issue [15–17]. Most of the works on CMLs so far were based on synchronous updating [18–24]. The occurrence of synchronous updating of events is rarely visible in natural systems. In general, the update of the units in a CML is made synchronously in contrary to the reality where, the elements in an array are not perfectly synchronous. Thus, some amount of asynchronocity is essential in modeling spatially extended complex systems. The degree of asynchronocity of a node can be defined as the probability of being not updated at each time step. Thus, the network with asynchronocity 0 is the standard synchronously updated

network. Therefore, increase of the parameter value indicates the increase of asynchronicity in the model. However, synchronocity parameter $q = k/N$ represents that k number of nodes among the total N nodes are updated at an instant. Hence, value of synchronocity parameter 1 corresponds to value 0 for asynchronocity parameter. Asynchronous updating may generate window of synchronized orbits and induce regularity in coupled systems [25–27].

In natural and artificial systems, asynchronous updating is common. Large scale integrated circuit design is an important field of application of asynchronous updating. Another good example of random asynchronous updating is social network [28]. In a cellular automata model, it has been shown that updating the model within a time step has a huge impact on the model output [29]. Some other asynchronously updated systems are multiprocessor systems, distributed digital networks, discrete time models of market economy etc. There are studies where CML evolve asynchronously i.e. where updates of lattice sites are sequential instead of being concurrent. Dynamics of asynchronous global maps have been studied using mean field approximation [30]. Neurons and neuron groups evolve asynchronously and thus employ asynchronous schemes. So, it is worth investigating the effects of asynchronocity on these models [31]. The issue of asynchronocity also appears in the context of boolean networks and biological networks. Monte Carlo algorithms which are used to simulate equilibrium statistical mechanical system uses asynchronous updating [32]. The similarities of delay dynamical network and asynchronously updated network have been discussed in a recent paper [33]. Recently, study of asynchronous stochastic updating [28, 34, 35] over networks have gained momentum due to its ability to model biological, social systems.

Mehta and Sinha [26] have reported the effects of asynchronous updating on the synchronization behavior of a CML. In their proposed updating rule they break the lattice into disjoint subsets, and update the sites belonging to each subset simultaneously, while updating different subsets sequentially. CML with asynchronous sequential updating are not suitable to model social and economic networks, neural networks, and gene or protein webs. However, CML with asynchronous stochastic updating [28] is more suitable to model such systems. These facts motivate us to report the synchronization behavior of CML with asynchronous stochastic updating of nodes. In case of stochastic asynchronous updating, at each time step, only some randomly chosen nodes are updated and others stay at their previous states.

In this work, we have investigated the impacts of stochastic asynchronous updating on the synchronization behavior of a CML in 1D and 2D models under nearest neighbor coupling with periodic boundary conditions. We have chosen the updating rule in such a way that a randomly chosen fraction of nodes will be updated at every time step. We discuss the effect of varying degree of asynchronocity on the synchronization behavior of the CML and speculate to match the results with the analytics. The section wise split of the paper is the following: in section 2, we formulate the model of CML with asynchronous updating. In section 3, we provide analytical as well as numerical results and discuss specific examples to elucidate the results. In section 4, an overall conclusion is drawn.

2. Model

The governing equations of CML with well known nearest neighbor interaction over a ring network [18] are the following

$$x_{n+1}(i) = (1 - \epsilon) f(x_n(i)) + \frac{\epsilon}{2}[x_n(i-1) + x_n(i+1)], \tag{1}$$

where $x_n(i)$ represents the state variable, $n(\geqslant 0)$ is the integer valued time index, $i = 1, \ldots N$ are the space index, N is the linear size of the array, ϵ is the coupling strength. In this model every node of the CML are updated synchronously.

To investigate the effectiveness of stochastic asynchronous updating on the synchronization behavior of a network of coupled maps we modify the above model and formulate the mathematical scheme as

$$\begin{aligned} x_{n+1}(i) = {} & (1 - \epsilon) f(x_n(i)) + \epsilon (g(x_n(i+1)) \\ & + g(x_n(i-1)))/2 \text{ for } i \in \Xi(n) \\ = {} & x_n(i) \text{ for } i \notin \Xi(n), \end{aligned} \tag{2}$$

where $\Xi(n)$ is the set of randomly chosen integers from the interval $[1, N]$ at time n. The elements of the set $\Xi(n)$ vary stochastically with time. $f(x)$ represents the local map, ϵ the coupling constant and $g(x)$ the coupling function which can take different forms. The impact of different degrees of asynchronocity can be realized taking more than one values from $\Xi(n)$ at each time step. On a 2D lattice the system looks like

$$\begin{aligned} x_{n+1}(i,j) = {} & (1 - \epsilon) f(x_n(i,j)) + \epsilon (g(x_n(i+1,j)) \\ & + g(x_n(i-1,j)) \\ & + g(x_n(i,j-1)) + g(x_n(i,j+1)))/4 \\ & \text{for } i \in \Xi(n) \\ = {} & x_n(i,j) \text{ for } i \notin \Xi(n). \end{aligned} \tag{3}$$

For more clarity, we assume to take k values at random out of N possibilities from the set $\Xi(n)$ at each time step and update those elements. The rest elements stay at their previous states. We define the degree of synchronocity q as $q = k/N$. Due to the random selection of nodes some nodes update more than other nodes.

The asynchronocity induced globally coupled map network the can be written as

$$\begin{aligned} x_{n+1}(i) = {} & (1 - \epsilon) f(x_n(i)) \\ & + \frac{\epsilon}{N-1} \sum_{\substack{j=1 \\ j \neq i}}^{N} f(x_n(j)) \text{ for } i \in \Xi(n) \\ = {} & x_n(i). \text{ for } i \notin \Xi(n). \end{aligned} \tag{4}$$

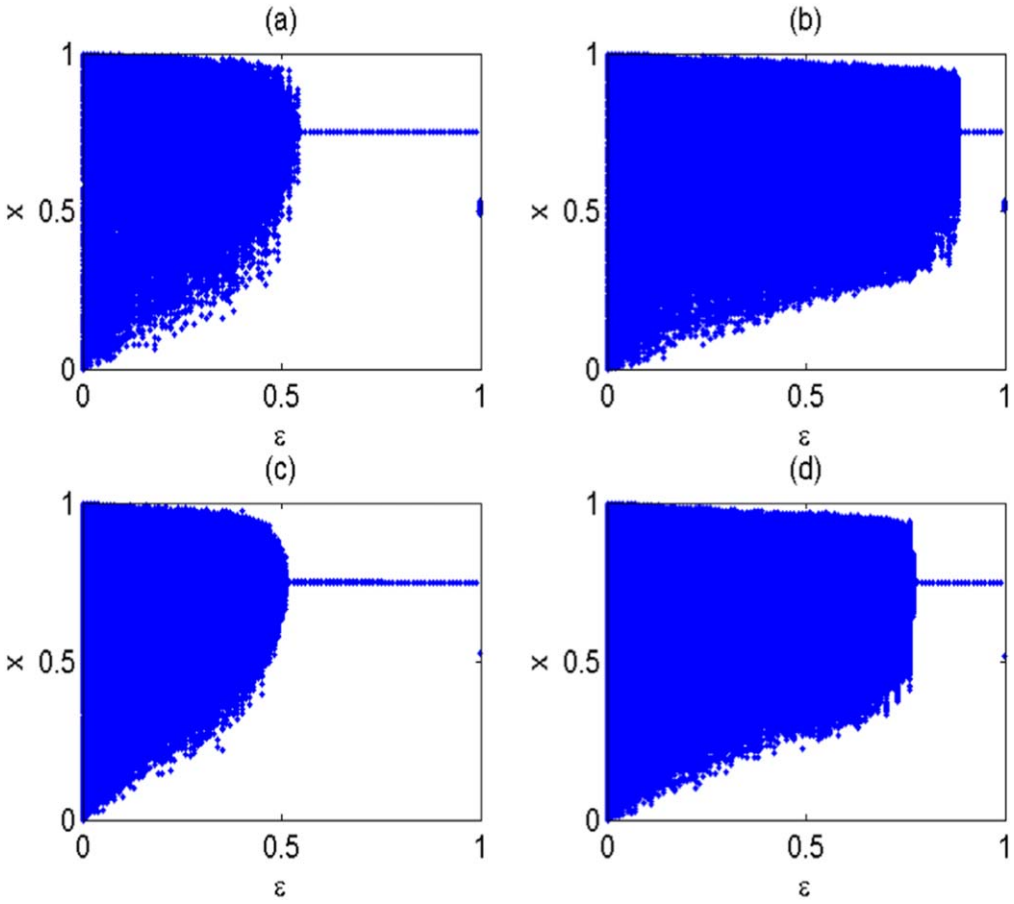

Figure 1. Bifurcation diagram of coupled logistic maps with $g(x) = x$ with respect to ϵ in 1D ring lattice for (a) $q = 0.6$, (b) $q = 0.95$ and in 2D lattice with periodic boundary conditions for (c) $q = 0.4$, (d) $q = 0.9$ under asynchronous updating.

In this paper, we choose nearest neighbor coupling and analyze the effect of asynchronocity in updating on the stability behavior. We attempt to realize how far the dynamics under asynchronous updating deviates from the synchronous case. In our present study, we choose one dimensional maps as local maps.

3. Results and discussion

3.1. Numerical results

For simulation, we have taken a ring lattice of 100 nodes for both 1D and 2D lattices and update each site asynchronously instead of synchronous evolution. We used different coupling forms like $g(x) = f(x)$ and $g(x) = x$ to check the effect of asynchronocity on the network synchronization behavior. The initial conditions are randomly chosen from the interval (0, 1) and the time steps are taken as 2000 with transient 1800. Our choice of nodes for updating is not sequential but random. Here, we vary the degree of asynchronocity $(1-q)$ of updating and check if the range of stable synchronized window changes with the variation of q.

We consider first a network of coupled chaotic logistic map

$$f(x) = 4x(1 - x)\, x \in [0, 1]$$

and update the sites asynchronously instead of updating simultaneously for numerical simulation. With increasing degrees of synchronocity (q), the number of updated nodes at a time increases and the limiting case $q = 1$ is our traditional synchronous case. Other extreme case $q = 0$ represents the evolution with no updating. We draw the bifurcation diagrams with respect to coupling strength of 1D and 2D CML with $g(x) = x$ for different values of synchronocity parameter q in figure 1. It can be observed that, a window of synchronized fixed point is generated for a wide range of coupling strength even for nearest neighbor interaction unlike the result of the synchronous case, where no synchronized window is found. The size of the window gradually shrinks with the increase in q, as can be seen in figure 1. From numerics, the ranges of synchronized fixed point orbit for 1D lattice with $q = 0.6$ is found to be $0.55 < \epsilon < 1$ (figure 1(a)) and that for $q = 0.95$ it is $0.89 < \epsilon < 1$ (figure 1(b)). For 2D lattice, the ranges of synchronization for different q values look similar to that of 1D lattice. Taking $q = 0.4$ and $q = 0.9$ we have drawn the bifurcation diagrams for 2D lattice in figures 1(c)

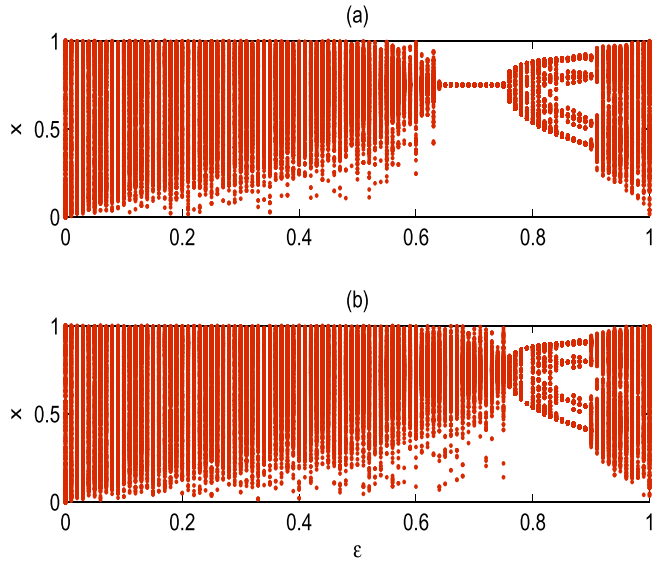

Figure 2. Bifurcation diagram of asynchronously updated coupled logistic maps with respect to ϵ in 1D ring lattice with $g(x) = f(x)$ for (a) $q = 0.5$, (b) $q = 0.6$.

and (d) respectively. For small values of q, the ranges do not vary much for both the cases of 1D and 2D lattice, rather keep the same range $0.54 < \epsilon < 1$.

Taking coupling function $g(x) = f(x)$, the bifurcation diagram for 1D ring lattice with respect to coupling strength exhibits fixed point window, as shown in figure 2. Figures 2(a) and (b) capture the synchronization behavior under asynchronous updating for $q = 0.5$ and $q = 0.6$ respectively. Synchronized fixed point window can be observed in figure 2(a) which disappears as the synchronocity parameter is slightly increased (figure 2(b)). More clearly speaking, as the value of q increases, the fixed point orbit loses its stability. We have noted that, only for $0 < q < 0.55$ the synchronized fixed point can be identified. Another important observation here is that, the right end value of the window of synchronization is the same for all values of q and that value is $\epsilon \simeq 0.74$.

Next we study the impact of the number of nodes on the synchronization behavior. If we increase the number of nodes in the lattice having coupling function $g(x) = f(x)$, the synchronization behavior changes slightly and these are captured in figure 3 for 1D lattice. For low number of nodes, synchronized period 2 orbit appears in some range of ϵ; e.g. $0.75 \leqslant \epsilon \leqslant 0.8$ for $N = 20$, which is depicted in figure 3(a). This period 2 window continues to appear for $N = 50$, as can be seen in 3(b). But, the synchronized period 2 orbit disappears as we move further to $N = 100$ (shown in 3(c)) and then to $N = 1000$ (plotted in 3(d)). A 2D lattice with periodic boundary conditions also shows the same behavior both qualitatively and quantitatively.

Furthermore we look on the influence of asynchronous updating on the network for other local maps. In figure 4, we have presented the bifurcation diagrams of 1D lattice with respect to coupling strength for different local maps and some chosen sets of map parameters and different degrees of asynchronocity. By plotting the bifurcation diagram of coupled Ricker maps

$$f(x) = xe^{4(1-x)}\, x \in [0, \infty)$$

in figure 4(a), with coupling function $g(x) = x$ for $q = 0.6$, we confirm our assertion that, asynchronocity can open up window of synchronized fixed point orbit. It is well known that cubic map

$$f(x) = -x^3 + 3x \tag{5}$$

shows bistability. For coupled cubic maps, bistable fixed points are generated. In figure 4(b), taking $q = 0.8$, the synchronization behavior of coupled cubic maps is featured for positive initial conditions (with blue color) and negative initial conditions (with magenta color) simultaneously. Taking coupled discontinuous maps

$$\begin{aligned} f(x) &= ax + \mu \text{ if } x < 0 \\ &= bx + \mu + c \text{ elsewhere,} \end{aligned}$$

(with a, b, μ being map parameters and c being the length of the gap of discontinuity) we have tested the effect of various types of stochastic asynchronocity and found that the results are qualitatively similar to the CML with smooth maps. Figure 4(c) displays bifurcation diagram with respect to coupling strength for coupled discontinuous maps with $a = -1.2$, $b = -1.3$, $\mu = -0.4$, $c = 0.55$ for $q = 0.5$ and positive initial conditions. Here also asynchronocity creates fixed point windows. We can reach to the same conclusion from figure 4(d), which is the bifurcation diagram of coupled discontinuous maps with $q = 0.9$ and negative initial conditions with the map parameters same as before.

If s number of random initial conditions are taken and among them synchronization are obtained in w cases, then the fraction of random initial conditions F, for which synchronization occurs in the lattice is defined as $\frac{w}{s}$. To compute the fraction of initial conditions (F) leading to synchronization of the fixed point of the network of coupled chaotic logistic maps with asynchronous updating, we have taken 100 random initial conditions. The value of F may lie between 0 and 1. If $w = s$, i.e $F = 1$ then synchronization happens in all cases. $F = 1$ implies complete synchronization and F less than 1 denotes partial synchronization or no synchronization. Figure 5 displays the fraction of random initial conditions which are attracted to the synchronized state in $\epsilon - q$ parameter space of 1D CML of chaotic logistic maps with coupling function $g(x) = x$ over ring network. With higher q the fraction tends to zero, indicating the destruction of synchronized fixed point orbits with the decrease of asynchronocity.

The point of onset of synchronization in parameter space ϵ_{bifur} is plotted in figure 6 for a 1D network of logistic maps over the ring network. The figure points out the fact that, for higher values of q the value of ϵ_{bifur} becomes larger. However, the value of ϵ_{bifur} decreases with the decrease of q and ϵ_{bifur} remains fixed after a critical value of q.

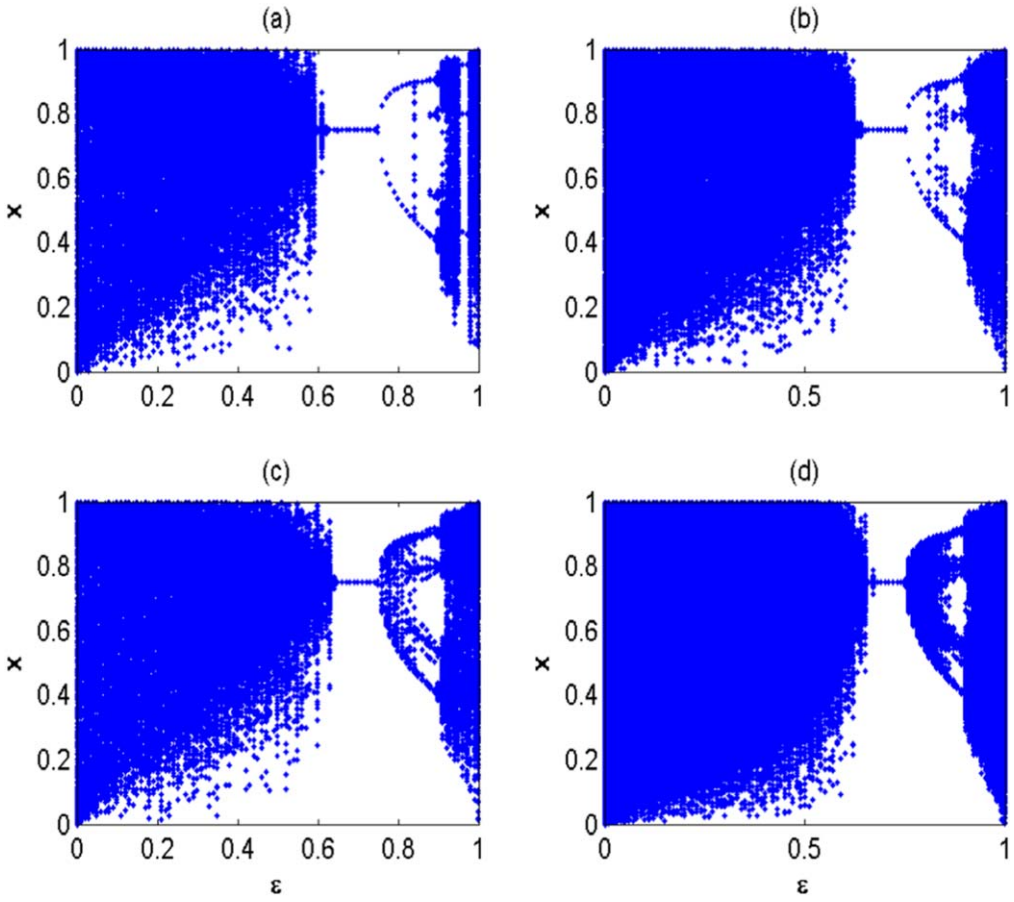

Figure 3. Bifurcation diagram of asynchronously updated coupled logistic maps with respect to ϵ in 1D ring lattice with $g(x) = f(x)$ for $q = 0.5$, with different number of nodes (a) $N = 20$, (b) $N = 50$, (c) $N = 100$, (d) $N = 1000$.

Finally we consider the globally coupled chaotic map as equation [4]. From the bifurcation diagram of globally coupled chaotic logistic map $4x(1-x)$ in figure 7(a), for $q = 0.6$ the range of synchronized fixed point window is found to be $0.51 < \epsilon < 1$. However for $q = 0.8$ no synchronized periodic window can be detected in figure 7(b).

3.2. Analytical results

Though due to the stochasticity in updating it is quite difficult to derive the exact analytical solution for the stability of the fixed point, we have tried to give some intuitive arguments for stability of such systems. For analytical calculation taking $g(x) = x$ in the system [2] the averaged out equation [18] can be written as

$$x_{n+1}(i) = q[(1-\epsilon)f(x_n(i)) + \frac{\epsilon}{2}\{x_n(i+1) + x_n(i-1)\}] + (1-q)x_n(i). \tag{6}$$

This equation can be written for higher values of q only. For lower q the case is far different. For stability analysis of the synchronized fixed point x^*, which is the period 1 orbit of the local map, we calculate the Jacobian matrix as

$$J = \begin{pmatrix} q(1-\epsilon)d + (1-q) & q\frac{\epsilon}{2} & 0 & \dots & 0 & q\frac{\epsilon}{2} \\ q\frac{\epsilon}{2} & q(1-\epsilon)d + (1-q) & q\frac{\epsilon}{2} & \dots & 0 & 0 \\ \vdots & \vdots & \vdots & \vdots & \vdots & \\ q\frac{\epsilon}{2} & 0 & 0 & \dots & q\frac{\epsilon}{2} & q(1-\epsilon)d + (1-q) \end{pmatrix}, \tag{7}$$

where, $d = \frac{df(x)}{dx}|_{x^*}$. As J is a circulant matrix, the eigenvalues of the matrix are given by

$$[q(1-\epsilon)d + (1-q) + q\epsilon\cos\theta_r] \text{ where, } \theta_r = 2\pi r/N$$

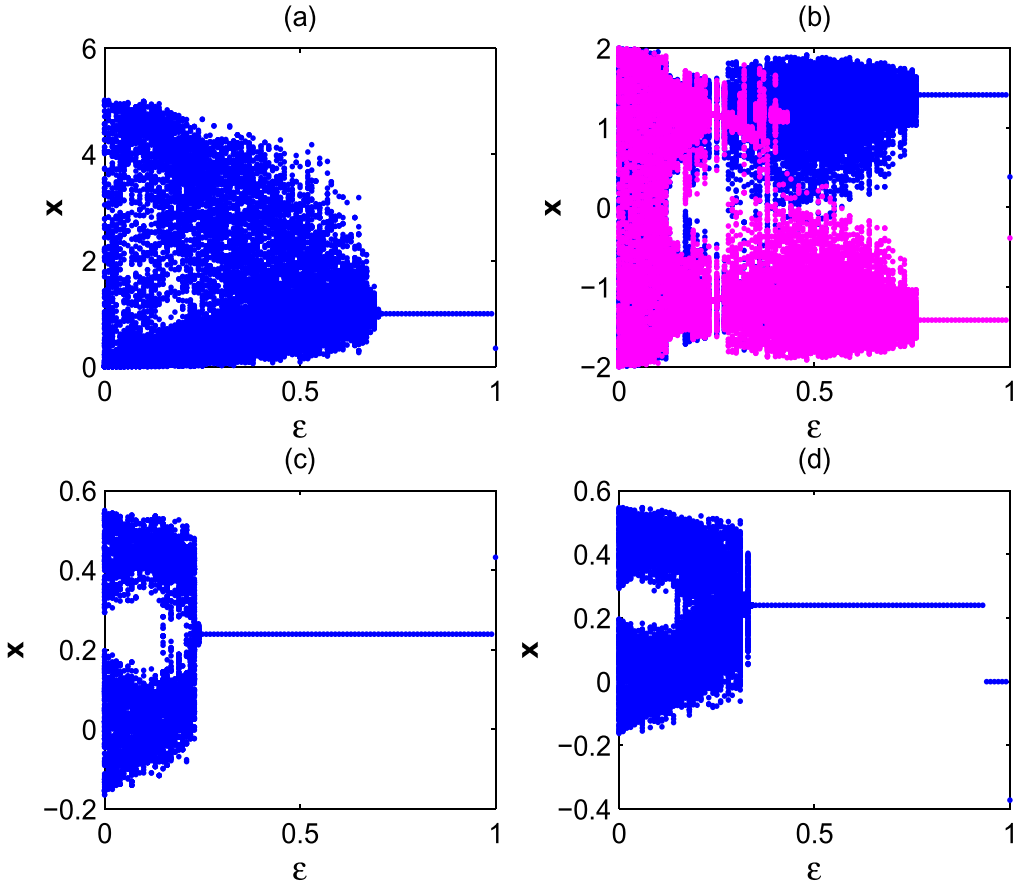

Figure 4. Bifurcation diagrams of asynchronously updated 1D lattice with respect to ϵ for different local map and $g(x) = x$ as coupling function; (a) coupled Ricker maps for $q = 0.6$, (b) coupled cubic map for $q = 0.8$ with both +ve (blue color) and −ve (red color) initial conditions, (c) coupled discontinuous maps with $a = -1.2$, $b = -1.3$, $\mu = -0.4$, $c = 0.55$ for $q = 0.5$ and +ve initial conditions and (d) with the same parameter sets as (c) for $q = 0.9$ and negative initial conditions.

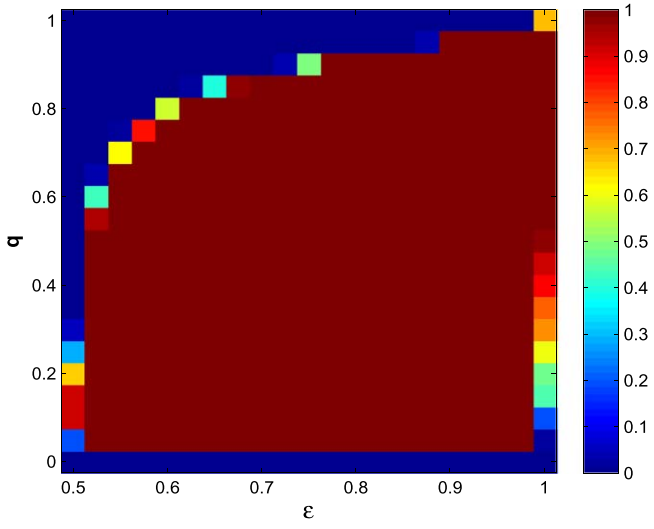

Figure 5. Density plot of fraction of initial states leading to synchronization in $\epsilon - q$ parameter space for 1D coupled logistic maps with $g(x) = x$ under asynchronous updating. The value 1 in colorbar represents complete synchronization.

$r = 0,\ 1,\ 2\ ...\ (N-1)$. The synchronized spatiotemporal fixed point will be stable if all eigenvalues of J lie inside the unit circle (centered at origin) in the complex plane. This makes the stability condition of the form

$$|[q(1-\epsilon)d + (1-q) + q\epsilon\cos\theta_r]| < 1.$$

After some simple calculations, we get the range of stability of the synchronized fixed point as

$$\frac{2}{q(1+d)} - \frac{1-d}{1+d} < \epsilon < -\frac{1-d}{1+d},\ \text{if}\ d < -1$$

and the inequality is reversed for the rest cases. Taking chaotic logistic map $f(x) = 4x(1-x)$ as local map and coupling function $g(x) = x$ for a high synchronocity $q = 0.9$, the range of synchronized periodic orbit is found to be $0.89 < \epsilon < 1$, that matches quite well with the numerical finding.

Now, taking coupling $g(x) = f(x)$, we can calculate the range of synchronized fixed point as well. Proceeding as above, we get the eigenvalues of the Jacobian matrix as

$$q(1-\epsilon)d + (1-q) + q\epsilon\ d\cos\theta_r \text{ where, } \theta_r = 2\pi r/N$$

$r = 0,\ 1,\ 2\ ...\ (N-1)$. Stability region is given by

$$\frac{(1-d)q-2}{-2qd} < \epsilon < -\frac{1-d}{2d},\ \text{if}\ d < 0$$

else, the inequality reverses. For chaotic coupled logistic maps $4x(1-x)$, the upper bound of the inequality is always

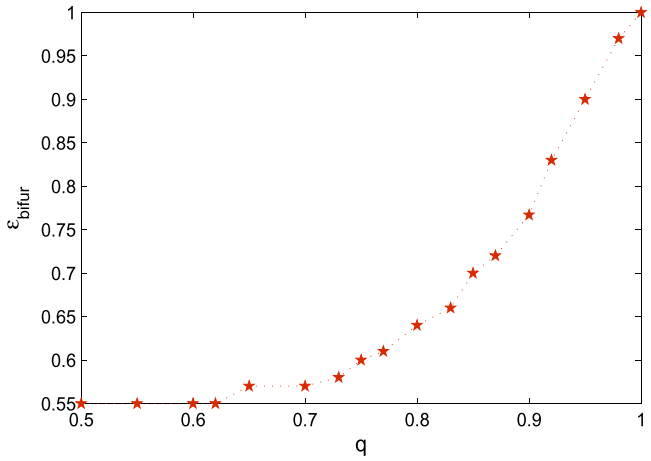

Figure 6. Variation of ϵ_{bifur} with the variation of q in 1D ring lattice with logistic maps taking $g(x) = x$ under asynchronous updating.

system [3] is as follows

$$x_{n+1}(i,j) = q[(1-\epsilon)f(x_n(i,j)) + \epsilon\ ((x_n(i+1,j)) + (x_n(i-1,j)) + (x_n(i,j-1)) + (x_n(i,j+1)))/4] + (1-q)x_n(i,j), \quad (8)$$

For stability analysis of the synchronized fixed point x^*, we can write the Jacobian as

$$J = \begin{pmatrix} A & B & 0 & \ldots & 0 & B \\ B & A & B & .... & 0 & 0 \\ \vdots & \vdots & \vdots & \vdots & \vdots & \\ B & 0 & 0 & \ldots & B & A \end{pmatrix}, \quad (9)$$

where,

$$A = \begin{pmatrix} q(1-\epsilon)d + (1-q) & q\frac{\epsilon}{4} & 0 & \ldots & 0 & q\frac{\epsilon}{4} \\ q\frac{\epsilon}{4} & q(1-\epsilon)d + (1-q) & q\frac{\epsilon}{4} & .... & 0 & 0 \\ \vdots & \vdots & \vdots & \vdots & \vdots & \\ q\frac{\epsilon}{4} & 0 & 0 & \ldots & q\frac{\epsilon}{4} & q(1-\epsilon)d + (1-q) \end{pmatrix}, \quad (10)$$

0.75 irrespective of the asynchronocity parameter value and this supports the results obtained from the numerics.

However, for lower values of q, the above analysis is unable to explain the dynamics of such systems. The reason behind such scenario can be understood following Atmanspacher [36]. For this, we consider the system for synchronous case

$$x_n(i+1) = (1-\epsilon)f(x_n(i)) + \frac{\epsilon}{2}\{x_n(i+1) + x_n(i-1)\}.$$

The stability of the fixed point solution requires the eigenvalue of the Jacobian matrix to stay within the unit circle. The eigenvalues take the form $(1-\epsilon)d + \epsilon\cos\theta_r$ with $\theta_r = 2r\ \ \pi/N$. Stability of fixed point demands $-1 < (1-\epsilon)d + \epsilon\cos\theta_r < 1$. Near the lower bound of stability equation the individual perturbation from the fixed point solution changes sign at each iteration at random. So on an average the contribution from the neighbors are expected to be canceled out. The stability condition now takes the form $-1 < (1-\epsilon)d$ which for $f(x) = 4x(1-x)$ becomes $0.5 < \epsilon$.

Even with 2D lattice the results do not seem to differ from the ring lattice behaviors. Considering a 2D lattice with asynchronous updating having local map as $4x(1-x)$ and coupling function $g(x) = x$, we can check our assertion. For higher q values, the averaged out equation coming from the where $d = \frac{df(x)}{dx}|_{x^*}$ and

$$B = \begin{pmatrix} q\frac{\epsilon}{4} & 0 & \ldots & 0 & 0 \\ 0 & q\frac{\epsilon}{4} & .... & 0 & 0 \\ \vdots & \vdots & \vdots & \vdots & \vdots \\ 0 & 0 & \ldots & 0 & q\frac{\epsilon}{4} \end{pmatrix}. \quad (11)$$

J is an $N^2 \times N^2$ block circulant matrix. The eigenvalues can be found using the properties of block circulant matrix by making it block diagonal. The block diagonal form is

$$D = \begin{pmatrix} M_0 & 0 & \ldots & 0 \\ 0 & M_1 & \ldots & 0 \\ \vdots & \vdots & \ldots & \vdots \\ 0 & 0 & \ldots & M_{N-1} \end{pmatrix}, \quad (12)$$

where the matrix $M_r (r = 0,\ 1,\ 2,\ \ldots N-1)$ are $N \times N$ matrices given by

$$M_r = A + 2B\cos\theta_r \quad (13)$$

and $\theta_r = 2\pi r/N$.

The individual matrix M_r is a circulant matrix. Thus the eigenvalues of J take the form

$$q(1-\epsilon)d + (1-q) + q\frac{\epsilon}{2}\cos\theta_r + q\frac{\epsilon}{2}\cos\theta_s$$

with $\theta_s = 2\pi s/N$.

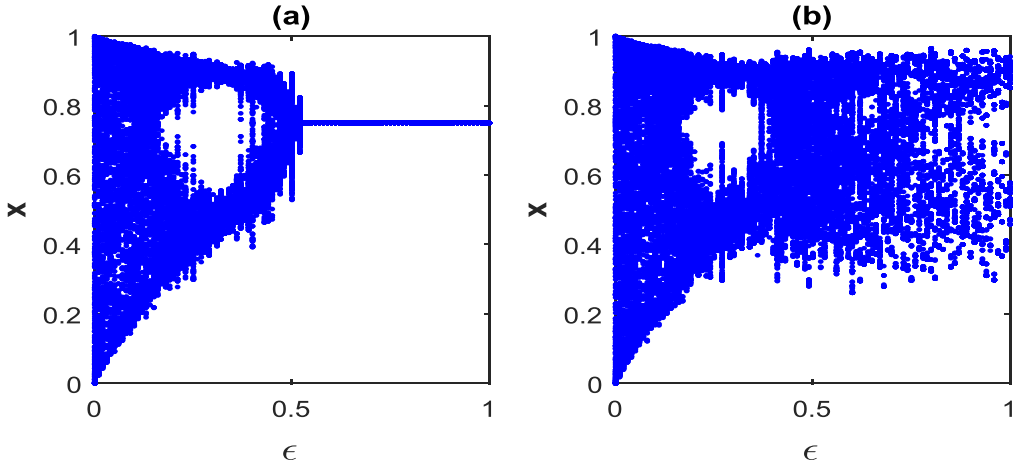

Figure 7. Bifurcation diagram of 1D globally coupled map under asynchronous updating for (a) $q = 0.6$ and (b) $q = 0.8$.

With different combinations of r and s, N^2 eigenvalues can be obtained. For stability, the norm of all eigenvalues must be less than unity. Maximum eigenvalue is $q(1-\epsilon)d + (1-q) + q\epsilon$ and minimum eigenvalue is $q(1-\epsilon)d + (1-q) - q\epsilon$. So the stability conditions are

$$\frac{2}{q(1+d)} - \frac{1-d}{1+d} < \epsilon < -\frac{1-d}{1+d}, \text{ if } d < -1$$

and the inequality is reversed for the rest cases. It can be noticed that the conditions are the same as derived from that of the 1D lattice described in equation [6].

For asynchronous globally coupled network as referred in equation [4] the evolution equation can be written as

$$x_{n+1}(i) = q[(1-\epsilon)f(x_n(i)) + \frac{\epsilon}{N-1}\sum_{\substack{j=1 \\ j\neq i}}^{N} f(x_n(j))] + (1-q)x_n(i). \quad (14)$$

For stability analysis of the synchronized fixed point x^*, we calculate the Jacobian as

$$J' = \begin{bmatrix} A' & B' & B' & B' & \dots & B' \\ B' & A' & B' & B' & \dots & B' \\ \vdots & \vdots & \vdots & \vdots & \dots & \vdots \\ B' & B' & B' & B' & \dots & A' \end{bmatrix}, \quad (15)$$

where $A' = q(1-\epsilon)f' + (1-q)$ and $B' = \frac{\epsilon}{N-1}qf'$, $f' = \frac{df(x)}{dx}|_{x^*}$. The eigenvalues can be written as

$$\begin{aligned} M_r &= A' + \omega_r B' + \omega_r^2 B' + ... + \omega_r^{N-1} B' \\ &= A + B(e^{i\theta_r} + e^{2i\theta_r} + ... + e^{(N-1)i\theta_r}) \\ &= A + Be^{i\theta_r}(1 - e^{i(N-1)\theta_r})/(1 - e^{i\theta_r}) \end{aligned} \quad (16)$$

$\omega_r = e^{i\theta_r}$, $\theta_r = 2\pi r/N$.

Now, $M_0 = A' + (N-1)B'$. Eigenvalue of M_0 is $q(f'-1) + 1$.

For stability $-1 < q(f'-1) + 1 < 1$. Taking $f(x) = 4x(1-x)$, we have $f' = -2$ and so the range of stability of synchronized fixed point becomes $-1 < -3q + 1 < 1$ and this gives the range of q as $q < 0.66$. Thus synchronized fixed point orbit is not possible for $q > 0.66$.

4. Conclusion

This paper is comprised of the spatiotemporal evolution of the CML under stochastic asynchronous updating incorporating various degrees of asynchronocity. Results show that, updating can have a profound effect on synchronization behavior. From the phenomenology, the effect of asynchronous updating in creating windows of fixed points and periodic orbit in parameter space is confirmed. Asynchronocity exhibits a huge difference in collective behavior when compared with the synchronous updating results of CML. In case of synchronous updating synchronization is impossible [18] for nearest neighbor coupling. In contrast, it has been shown here that stochastic asynchronous updating can induce synchronization in network under purely nearest neighbor coupling. The results are verified numerically for smooth as well as nonsmooth maps. Even small asynchronocity is able to suppress the chaotic dynamics of the network and generate synchronization window. On the other hand, with the decrease of asynchronocity the range of synchronized fixed point shortens gradually. Analytic investigation supports the numerical results up to some extent, specifically for large values of q. Taking coupling function $g(x) = f(x)$, synchronized periodic orbit can be obtained for small values of q only. Lattice size is also an important factor if we consider coupling function $g(x) = f(x)$ and the nature of synchronized orbit depends strongly on the lattice size in this case. Synchronized period 2 appears for some ranges in the parameter space for smaller lattice size, which disappears with the increase of nodes. Therefore, we can conclude that synchronous and stochastic asynchronous updating may lead to qualitatively very different dynamics in case of nearest neighbor coupling. In globally coupled network synchronized fixed point generates for certain range of q but the size of periodic window does not vary with variation of ϵ. The study of asynchronous updating is motivated by the modeling of evolution of complex social, economical and physical systems and thus at the end asynchronocity emerge as a chaos controlling method for spatially extended dynamical systems. This study may be useful to explain the spatiotemporal order

structure observed in spatially extended biological and social systems by using asynchronous diffusion processes. Effects of variation of time scales of diffusion in the synchronization behavior of modular networks are open areas for further investigations.

Conflict of Interest

The authors declare that there is no conflict of interest.

ORCID iDs

Swarup Poria https://orcid.org/0000-0002-7804-6741

References

[1] Kaneko K 1993 *Theory and Applications of Coupled Map Lattices* (New York: Wiley)
[2] Hansel D and Sompolinsky H 1992 *Phys. Rev. Lett.* **68** 718
[3] Kamal N K and Sinha S 2015 *Pramana* **84** 249–56
[4] Winful H G and Rahman L 1990 *Phys. Rev. Lett.* **65** 1575
[5] Pecora L M, Carroll T L, Johnson G A, Mar D J and Heagy J F 1997 *Chaos* **7** 520
[6] Pikovsky A, Rosenblum M and Kurths J 2003 *Synchronization: A universal Concept in Nonlinear Sciences* (Cambridge: Cambridge University Press)
[7] Garcia-Morales V 2016 *J. Phys. A: Math. Theor.* **49** 295101
[8] Chate H and Manneville P 1991 *Europhys. Lett.* **14** 409
[9] Adachi S, Peper F and Lee J 2004 *Physica* D **198** 182–96
[10] Kaneko K 1989 *Physica* D **34** 1
[11] Schöll E and Wacker A 1995 *Nonlinear Dynamics and Pattern Formation in Semiconductors and Devices* (Heidelberg: Springer)
[12] Hadley P, Beasley M R and Wiesenfeld K 1988 *Phys. Rev.* B **38** 8712
[13] Kuramoto Y 2012 *Chemical Oscillations, Waves and Turbulence* (Berlin: Springer)
[14] Winfree A T 2001 *The Geometry of Biological Time Springer* (Heidelberg: Science and Business Media)
[15] Kundu P, Hens C, Barzel B and Pal P 2018 *Europhys. Lett.* **120** 40002
[16] Prasad A 2010 *Chaos Solitons Fractals* **43** 42–6
[17] Palaniyandi P and Rangarajan G 2017 *Sci. Rep.* **7** 8921
[18] Sinha S 2002 *Phys. Rev.* E **66** 016209
[19] Poria S, Khan M A and Nag M 2013 *Phys. Scr.* **88** 015004
[20] Marti A C and Masoller C 2003 *Phys. Rev.* E **67** 056219
[21] Atay F M, Jost J and Wende A 2004 *Phys. Rev. Lett.* **92** 144101
[22] Nag M and Poria S 2015 *Chaos* **25** 083114
[23] Nag M 2017 *Indian J. Phys.* **91** 1589–97
[24] Vasegh N 2017 *Nonlinear Dyn.* **89** 1089
[25] Lumer E D and Nicolis G 1994 *Physica* D **71** 440–52
[26] Mehta M and Sinha S 2000 *Chaos* **10** 350–8
[27] Rolf J, Bohr T and Jensen M H 1998 *Phys. Rev.* E **57** R2503
[28] Greil F and Drossel B 2005 *Phys. Rev. Lett.* **95** 048701
[29] Cornforth D, Green D G, Newth D and Kirley M 2002 *Proc. Artificial Life VIII—the 8th Int. Conf. or the Simulation and Synthesis of Living Systems (Sydney, Australia, 9–13 December)* pp 28–32
[30] Abramson G and Zanette D H 1998 *Phys. Rev.* E **57** 4572
[31] Shrimali M D, Sinha S and Aihara K 2007 *Phys. Rev.* E **76** 046212
[32] Swendsen R H and Wang J S 1987 *Phys. Rev. Lett.* **58** 86
[33] Gonzâlez-Avella J C and Anteneodo C 2016 *Phys. Rev.* E **93** 052230
[34] Luo C, Wang X and Liu H 2014 *Sci. Rep.* **4** 7522
[35] Luo C and Wang X 2013 *PloS One.* **8** e66491
[36] Atmanspacher H, Filk T and Scheingraber H 2005 *Euro. Phys. J.* B **44** 229–39